

S & M 0673

Tactile Sensor for Compliance Detection

Ahmed M. R. Fath El-Bab*, Mohamed E. H. Eltaib,
Mohamed M. Sallam and Osamu Tabata¹

Department of Mechanical Engineering, Assiut University, Assiut, Egypt

¹Department of Micro Engineering, Graduate School of Engineering, Kyoto University,
Yoshida-Honmachi, Sakyo-ku Kyoto, 606-8501 Japan

(Received January 10, 2007; accepted May 8, 2007)

Key words: tactile sensor, compliance detection, soft tissue

A macroscale tactile sensor using a resistance-type strain gauge is presented to demonstrate the concept of applying two sensors with considerably different stiffnesses to soft tissue for compliance detection. The design procedure for the tactile sensor was carried out. The sensor contains two cantilevers with different stiffnesses. One important advantage of the sensor is that its reading does not depend on the applied displacement between the sensor and the specimens. The measuring range of the sensor is 0–500 N/m, to cover a wide range of soft-tissue stiffnesses. Test specimens with stiffness constants of 60, 117, 174, and 480 N/m were used to test the sensor. The results showed that the sensor could distinguish the difference in stiffness of test samples under various applied loads. Eventually, this sensor is expected to be miniaturized by micro machining for use in medical applications.

1. Introduction

Today, much attention is given to tactile sensing in minimally invasive surgery.⁽¹⁾ In such surgery, it is of concern that much of the tactile information available in open surgery will be lost. Artificial tactile sensing can restore some of this lost tactile information. Also, artificial tactile sensing is very useful for clinicians who depend on their sense of touch in many physical examinations. They usually use palpation for routine diagnosis and during conventional surgical procedures. An artificial tactile sensor is a means of objectively measuring tissue properties. It could be used for the detection of cancerous lumps or for determining the health of a tissue. The aim of this project is to design and fabricate a tactile sensor for compliance detection to be used in medical applications such as: minimally invasive surgery (MIS), telesurgery, and remote palpation for remote physical examination. As a first step in this project, a macroscale

*Corresponding author: e-mail: ahmed_rashed@yahoo.com

tactile sensor is developed, on the basis of the concept of applying two sensors with considerably different stiffnesses to soft tissue for compliance detection, to demonstrate the ability of this concept in detecting the stiffness of a soft tissue independently on the applied displacement between the sensor and the tissue.

2. Materials and Methods

2.1 Tactile sensor design procedure

Step 1: Choose the property that will present the tissue compliance. In the applications of compliance detection by Omata and Terunuma⁽²⁾ and Sedaghati *et al.*,⁽³⁾ the modulus of elasticity E [N/m²] was selected as the mechanical property to represent the compliance. On the other hand, Engel *et al.*⁽⁴⁾ and Shikida *et al.*⁽⁵⁾ selected the stiffness K [N/m] instead. In this work, stiffness is chosen for representing the compliance, because the compliance could be defined simply as $(1/K)$ and that K could be more easily tactually displayed than the modulus of elasticity E . Furthermore, Sedaghati *et al.*⁽³⁾ concluded that there is a direct relationship between the local E and K , i.e., E is equal to K multiplied by a constant.

Step 2: Choose the sensor measuring range. Many scientists have studied the force-displacement relationship in human and animal soft tissue to extract data for the tissue stiffness or even elasticity, in order to use it in finite element analysis (FEA) or for the computer simulation of soft tissue, which is very useful in surgery simulation for training. Carter *et al.*⁽⁶⁾ plotted the stress-strain curve from an indentation test using a single-point compliance probe on the right lobe of the liver in five patients during open surgery. Four patients had a normal liver and the fifth patient had an abstractive liver disease. The results showed that the normal livers and the diseased liver had stiffnesses of 40 and 80 N/m, respectively. Therefore, the idea of differentiation between healthy and diseased tissue developed. Oleg *et al.*⁽⁷⁾ presented a study evaluating the effects of visual and haptic feedback on human performance in a needle insertion task. The stiffness values used for skin, fat, and muscle simulation are 331, 83 and 497 N/m, respectively. Chinzei *et al.*⁽⁸⁾ showed experimentally that the stiffness of swine brain is about 80–100 N/m and the Young's modulus is 7425 N/m². Farshad *et al.*⁽⁹⁾ performed a series of aspiration experiments using a pig's kidney; the results showed that the Young's modulus of the pig's kidney is 43500 N/m². Kim *et al.*⁽¹⁰⁾ developed a system for measuring the mechanical properties of soft tissue of a pig *in vivo* using a robotic device fitted with a force transducer, and the response of the liver and the lower esophagus was measured. The results showed that stiffness of the liver and the esophagus were 127 and 195 N/m, respectively. The Young's moduli reported were 31800 N/m² for the liver and 48800 N/m² for the esophagus. In accordance with the above review, the range of the sensor is selected to be 0–500 N/m to cover the stiffness values of the soft tissue organs.

Step 3: Choose the tactile sensor concept. Carter *et al.*⁽⁶⁾ have developed a probe for tissue characterization based on sensing the static force applied to the tissue and the corresponding tissue deformation or deflection. By this means, the stiffness could be quantified. The same approach is also used by Zheng and Mak⁽¹¹⁾ to assess the biomechanical properties of soft tissue. Husegawa *et al.*⁽¹²⁾ proposed a multifunctional

tactile sensor device driven by a magnetic force. The device has the advantage of the ability to detect multiple physical values, such as contact force and the elastic and damping coefficients of an object in contact with the sensor. The same team previously used an external pneumatic system for actuating the device, and confirmed that it can measure the elastic coefficient of an object (the stiffness).⁽⁵⁾ The problem of these approaches is that they always need an actuation force, and sometimes this force should be constant in order to differentiate between tissues by measuring the equivalent displacement. The extra device necessary to apply the constant force makes the sensor more expensive. Also, a reference point to measure the displacement may be needed in some designs, which makes a fixed frame essential for use as a reference point. All these make such a concept of limited use as a sensor attached to a probe freely held in the hand for medical applications.

Omata and Terunuma⁽²⁾ utilized an approach for the elasticity detection of soft tissue that involves the use of a piezoelectric ceramic as a transducer. The transducer applies vibration at its resonant frequency. When the free end of the probe touches a material, the resonant frequency shifts because of the acoustic impedance change. The shift in resonant frequency depends on the elasticity of the material. The main problems of this sensor are that it requires the application of a constant contacting force against an object of few grams and slow time response.

Eltaib⁽¹³⁾ developed a tactile probe based on the principle of subjecting the material to periodic oscillation and measuring the response of the tissue. By calculating the gain and the phase of the system at certain frequencies, the stiffness and the damping parameters could be identified. Although this approach could identify the stiffness and the damping parameters, it has the disadvantage that the sensor requires an actuation system to apply constant displacement.

Engel *et al.*⁽⁴⁾ developed a passive micromachined polyimide hardness sensor that does not rely on actuation and is based on signals from two sensors with considerably different stiffnesses. The proposed model assumed that the far-field displacement on the two spring stacks is the same. This sensor uses two polymer mesa structures for measuring springs: one is on the membrane and the other is on the bulk substrate, as shown in Fig. 1(a). The pressure ratio, (p_{mod}) at the interface of the reference and measurement springs (k_r and k_m) with the tissue, is a function of contact object hardness (k_{obj}), as shown in Fig. 1(b). A plot of this model over a range of object hardnesses relative to polyimide hardnesses is shown in Fig. 1(b).

Despite the theoretical model implies that the reading of the sensor does not depend on the contact force, the experiment results showed it is highly dependent on the applied force. This dependence of the outputs on the applied pressure might be attributed to the nonlinearity of the spring design (diaphragm with wide mesa). This nonlinearity might be resulted from the fact that the contact pressure between the sensor diaphragm and the tissue varies during loading. Also, many factors, e.g. crosstalk of the tissue, may be involved.

The authors chose the principle proposed by Engel *et al.* because of its advantage that it does not rely on actuation. The improvement in the implementation of the principle will be discussed in §2.2.2.

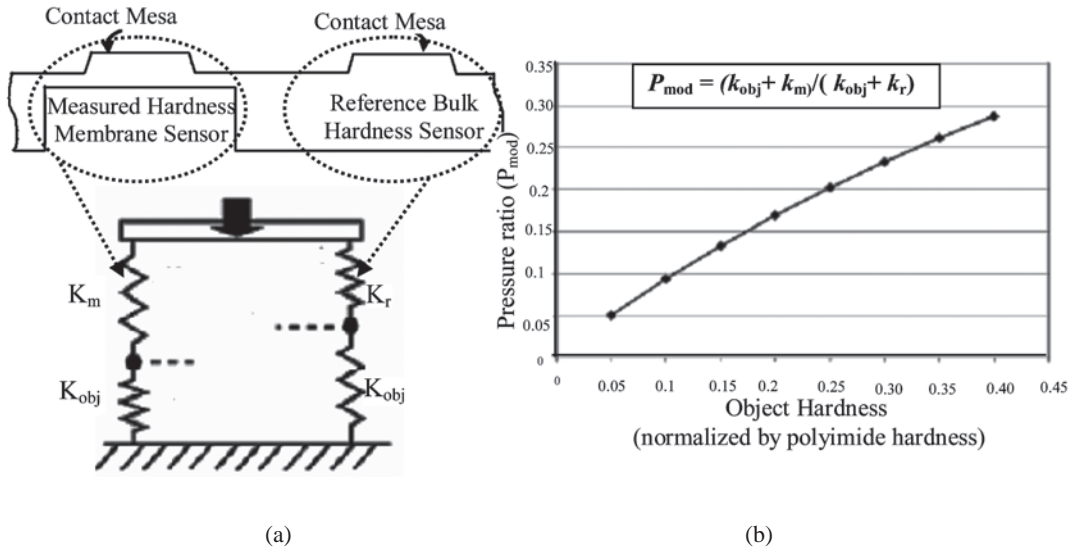


Fig. 1. Two-spring-based hardness sensor.

Step 4: Choose the transducer technology. Transducer technology may be capacitive, piezoresistive or piezoelectric. In the proposed macroscale sensor, a strain gauge was used because of its availability, its low cost and its relatively simple signal conditioning.

2.2 Proposed macroscale tactile sensor

2.2.1 Mathematical Model

The developed tactile sensor is modeled as shown Fig. 2(a). Although in the real case the soft tissue stiffness is nonlinear, it can be considered as linear under a small applied displacement.⁽¹⁴⁾ In this model, it is assumed that the soft tissue is of linear elasticity with stiffness k_o . It is also assumed that the far-field displacements X_H and X_L on the two spring stacks shown in Fig. 2(b) are the same.

Since $X_H = X_L$,

$$\frac{F_H}{K_H} = \frac{F_L}{K_L}$$

$$\therefore \frac{F_H}{F_L} = \frac{K_H}{K_L} = \frac{k_h(k_o + k_l)}{k_l(k_o + k_h)} = Q, \tag{1}$$

where F_H is force at spring K_h , F_L is force at spring K_l , K_H is equivalent spring stiffness of the high-stiffness side, K_L is equivalent spring stiffness of the low-stiffness side, k_o is object stiffness, k_h is stiffness of the high-stiffness sensor, k_l is stiffness of the low-stiffness sensor, and Q is force ratio.

Using eq. (1), the value of the object stiffness is expressed as follows:

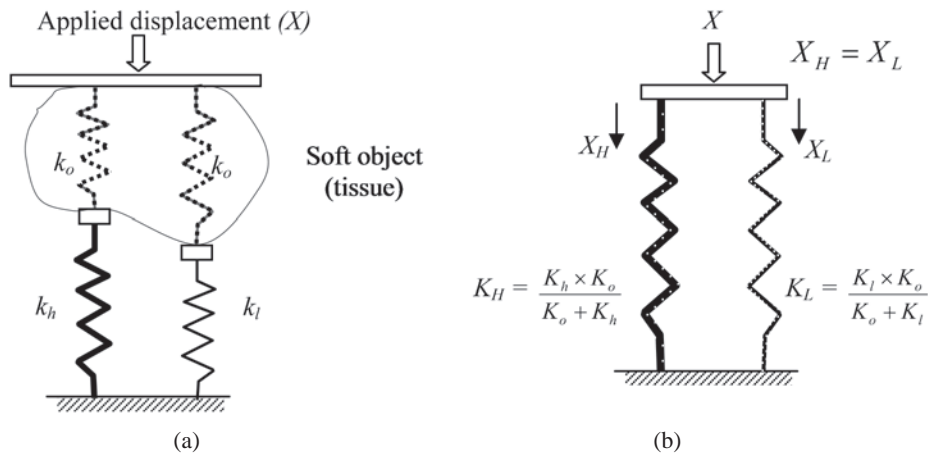


Fig. 2. Principle of applying two sensors with different stiffnesses to the tissue.

$$\therefore K_o = \frac{K_h \cdot K_l (1 - Q)}{(Q \cdot K_l - K_h)} \quad (2)$$

Thus, by knowing Q , the object stiffness k_o can be calculated. The most important advantage of this concept compared with the other concepts is that the value of the measured object stiffness k_o does not depend, theoretically, on the applied displacement or the total force applied by hand during the indentation of the soft tissue.

2.2.2 Sensor structure

The proposed sensor shown in Fig. 3 consists of two cantilever beams with the same length, but different thicknesses representing two springs with different stiffnesses. A cylindrical mesa on each cantilever allows the applied force to be concentrated at the free end of the cantilever during loading. Therefore, this design avoids the generation of distributed pressure on the cantilever, which ensures the linearity of the spring characteristics. The advantage to this design comparing to Engel's is that the object stiffness k_o is calculated from concentrated force ratio, which generated on the high- and low-stiffness springs. The ratio of concentrated forces (Q) is hopefully constant during pushing the sensor toward the tissue. In order to demonstrate this fact, two springs will be designed in the next section.

2.2.3 Optimization analysis

In this section an analytical procedure is followed to give reasonability for the selected sensor dimensions. To design the two cantilever beams, we have to take into account some restrictions. The value of sensitivity (dQ/dk_o) during the measuring range should be as large as possible to realize high accuracy when calculating the object stiffness k_o , but the following must be considered:

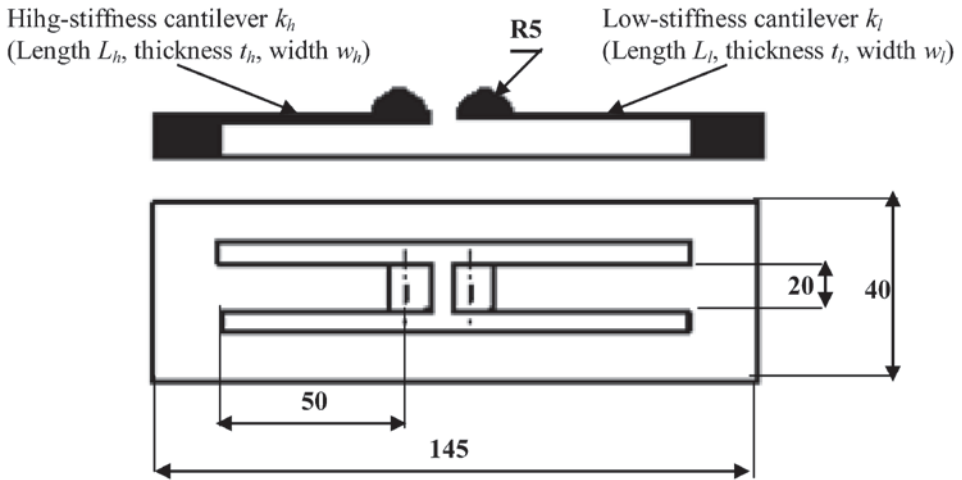


Fig. 3 Proposed prototype of the sensor.

1. The strains at the fixed end of both beams should be as equal as possible throughout the measuring range to ensure the accuracy of the measurement by obtaining a certain output voltage change from both beams which depends on the strain.
2. The difference between the deflections of both beams should not be large to avoid the crosstalk of the tissue, which affects the reading of the object stiffness k_o , as schematically shown in Fig. 4. The cross talk of the tissue is represented by horizontal spring k_c , assuming isotropic tissue. Detailed study of cross talk is one of our future works (out of scope of this paper).

As seen from eq. (1), the force ratio Q is a function of (k_o, k_h, k_l) , where:

$$k_h = \frac{E_h w_h t_h^3}{4L_h^3} \tag{3}$$

$$k_l = \frac{E_l w_l t_l^3}{4L_l^3} \tag{4}$$

E, w, t and L denote the Young's modulus, width, thickness, and length of the beam, respectively. The subscripts l and h denote low- and high-stiffness, respectively, as shown in Fig. 3.

In order to simplify the analysis, it is assumed that

- 1) $L_l = L_h = L$
- 2) E_l and E_h are equal to $E = 3 \times 10^9$ N/m² (perspex)
- 3) w_l and w_h are equal to 10 mm.

We now discuss the effect of changing the thickness of the two beams to control the Q value, the strain and deflection of both beams.

First, consider the sensitivity. From eq. (1):



Fig. 4. Crosstalk (shown by a horizontal spring between two vertical springs).

$$\frac{dQ}{dk_o} = \frac{k_h(k_h - k_l)}{k_l(k_o + k_h)^2}, \quad (5)$$

where dQ/dk_o represents the sensitivity of the change in Q due to the change in k_o . This value is positive, i.e., the sensitivity increases when $k_h/k_l > 1$. Since k_l and k_h depend only on the thickness (the other parameters are equal), $t_h/t_l > 1$. Therefore, when the ratio t_h/t_l increases, dQ/dk_o also increases (the sensitivity improves).

Second, consider the strains at the fixed end of both beams:

$$\varepsilon_l = \frac{6F_l L_l^3}{Ewt_l^2} \quad (6)$$

$$\varepsilon_h = \frac{6F_h L_h}{Ewt_h^2}, \quad (7)$$

where ε_l and ε_h are the strains at the fixed end of the low- and high-stiffness cantilever beams, respectively.

$$\frac{\varepsilon_l}{\varepsilon_h} = \frac{1}{Q} \left(\frac{t_h}{t_l} \right)^2 \quad (8)$$

Third, consider the deflections of both beams:

$$\Delta_l = \frac{4F_l L_l^3}{Ewt_l^3} \quad (9)$$

$$\Delta_h = \frac{4F_h L_h^3}{Ewt_h^3}, \quad (10)$$

where Δ_l and Δ_h are the deflections of the low- and high-stiffness cantilever beams, respectively.

$$\therefore \frac{\Delta_l}{\Delta_h} = \frac{1}{Q} \left(\frac{t_h}{t_l} \right)^3 \quad (11)$$

Substituting eq. (8) into eq. (11), we obtain the following relationship.

$$\frac{\Delta_l}{\Delta_h} = \left(\frac{\varepsilon_l}{\varepsilon_h} \right) \left(\frac{t_h}{t_l} \right) \quad (12)$$

Because the ratio $\varepsilon_l/\varepsilon_h$ is supposed to be equal to one during the measuring range, see restriction 1, the ratio between the two cantilever deflections Δ_l/Δ_h increases with increasing the thickness ratio t_h/t_l , as seen in eq. (12), which will strongly affect the accuracy of the measurement of k_o because of crosstalk as shown in Fig. 4. Therefore, as a compromise to obtain higher sensitivity and lower crosstalk, the ratio of t_h/t_l was chosen to be 3 ($t_h=3$ mm and $t_l=1$ mm). As it is seen, in this station of procedure t_h/t_l can be of any dimensions. In other words, t_h/t_l may be (3 mm / 1 mm) for macroscale sensor or (3 μm / 1 μm) in the miniaturized version.

Next, a study of the effect of changing the cantilever length was carried out using the above thickness ratio of 3. Substituting eqs. (3) and (4) into (1):

$$Q = C_1 \left(\frac{Lk_o + C_2}{Lk_o + C_3} \right), \quad (13)$$

where

$$C_1 = \left(\frac{t_h}{t_l} \right)^3, \quad C_2 = 3E_l I_l, \quad C_3 = 3E_h I_h.$$

Because of $C_2 < C_3$, the value in brackets in eq. (13) increases, and subsequently Q increases with increasing L . Considering eqs. (8) and (11), when the length increases, and subsequently Q increases, both the strain ratio and the deflection ratio decrease.

In order to verify these dependences, a comparison among three lengths of the cantilever beams of the sensor, namely $L = 40, 50,$ and 60 mm, was carried out. Figure 5 shows that Q increases with increasing L . Also, Fig. 6 shows that the strain ratio decreases with increasing L , which is beneficial for obtaining higher accuracy.

Although the deflection ratio decreases with increasing L , see eqs. (11) and (13), Fig. 7 shows that the deflection values of the two beams increase. As described previously, from the viewpoint of crosstalk, shorter beams are better, and give smaller deflection. From the above consideration, $L=50$ mm is chosen as a compromise between higher sensitivity and lower crosstalk.

3. Experimental Setup

The experimental setup shown in Fig. 8 contains a handle, which allows the specimen to be moved closer to the sensor, a displacement gauge and a base for fixing the sensor. Each Perspex specimen contains two cantilever beams of equal stiffness. For all specimens beams, thickness and width are 2 and 10 mm, respectively. By changing the

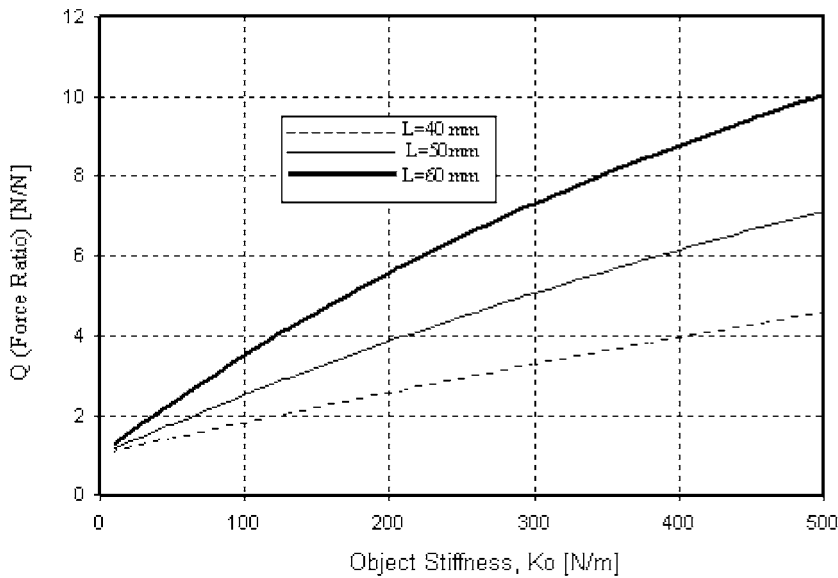


Fig. 5. Q value for different lengths of beams in the working range.

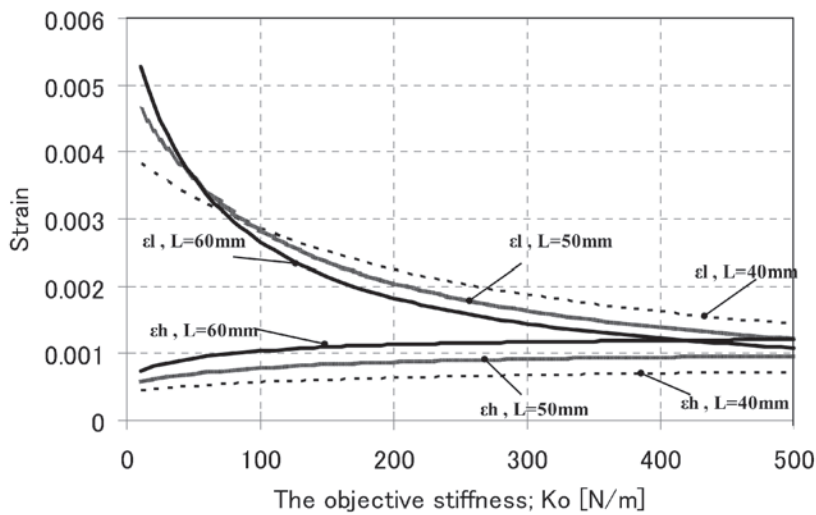


Fig. 6. Strain for both beams of different lengths in the working range.

length of the specimen, different stiffnesses could be created. The length and stiffness of four specimens created are summarized in Table 1. The specimens are chosen as two spring explicitly, not a real tissue or a silicone rubber, to get results not affected with crosstalk, and eventually, demonstrate the concept.

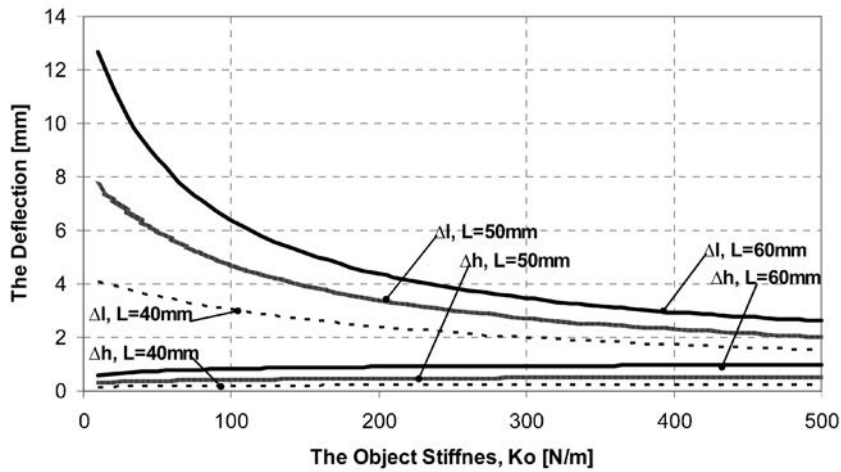


Fig. 7. Deflection for both beams of different lengths in the working range.

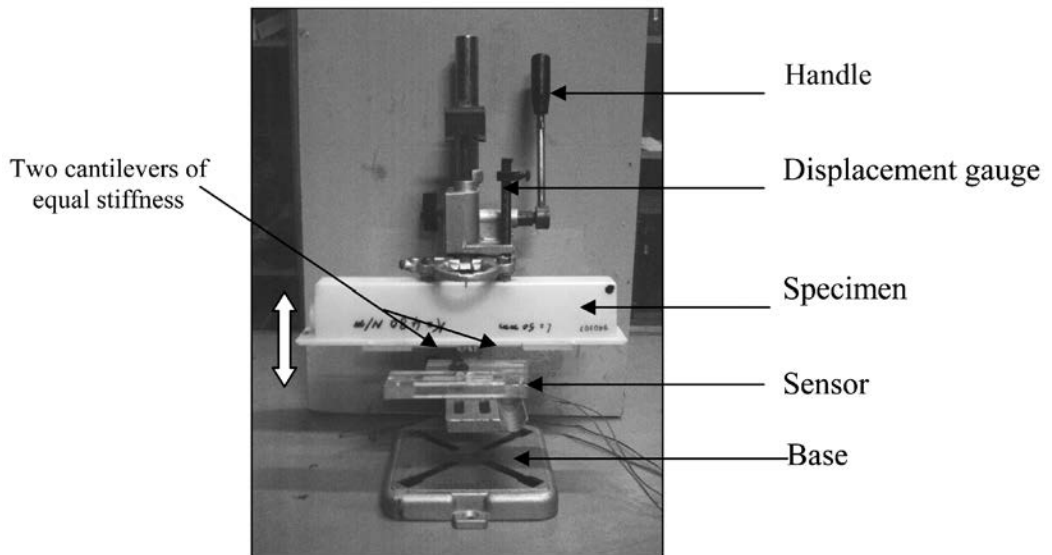


Fig. 8. Overall view of the experimental setup.

As shown in Fig. 9, each cantilever has a half-bridge strain gauge circuit. A strain-gauge amplifier amplifies the signal. Then, the analogue signal is converted to digital using an AD/DA Card and stored in a computer. A C-language program is adapted to record 1000 readings and their average for every 1 mm displacement of the specimen. In order to reduce the effect of the fluctuation of the readings, all readings more than three standard deviations from the mean value were rejected.

Table 1
Specimen lengths and their equivalent stiffnesses.

Specimen length (mm)	100	80	70	50
Equivalent specimen stiffness (N/m)	60	117	174	480

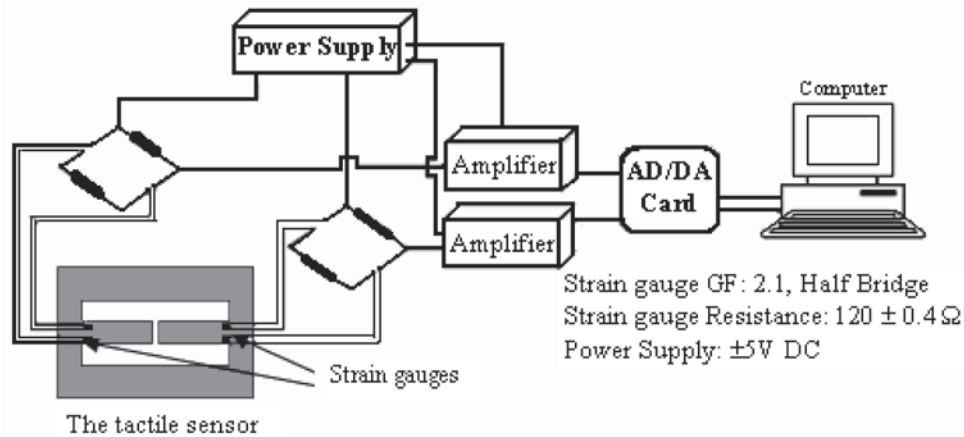


Fig. 9. Overall view of the measuring circuit.

Table 2
Mean reading of the sensor for each specimen.

Specimen no.	1	2	3	4
Theoretical stiffness K (N/m)	60	117	174	480
Mean reading of the sensor (N/m)	72	123	183.3	443

4. Results

Table 2 shows the mean reading of the sensor for the four known specimens with applied displacements from 0 to 8 mm. As shown in Fig. 10, the sensor can distinguish the four different stiffnesses. The readings were independent of the applied displacement between the sensor and the specimen.

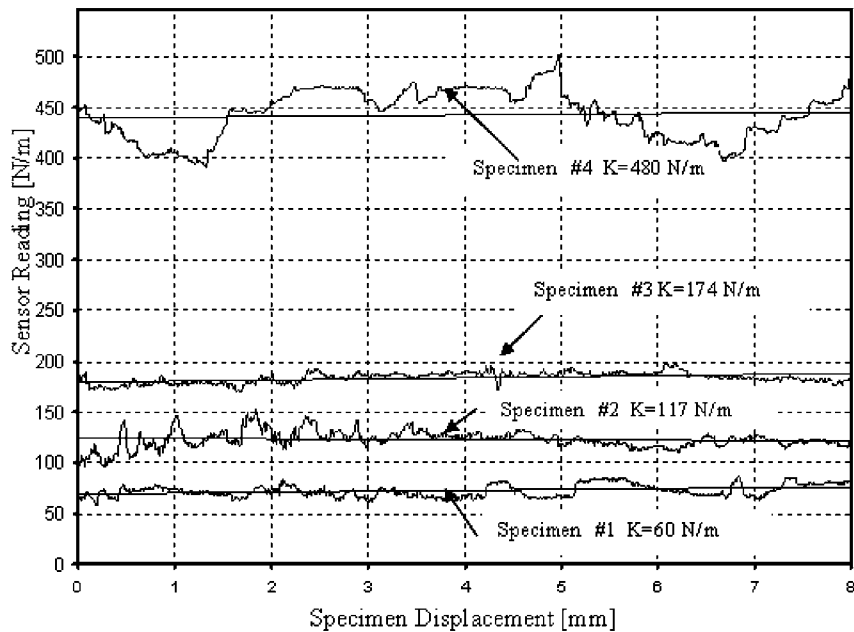


Fig. 10. Sensor reading for each specimen.

5. Conclusion

The design, fabrication and testing of a resistance-based macroscale tactile sensor are carried out to demonstrate the concept of applying two sensors of considerably different stiffnesses to soft tissue for compliance detection. The results show that the sensor can distinguish among different stiffnesses. One important and unique advantage of the sensor is that its reading does not depend on the applied displacement between the sensor and the specimen. This concept is demonstrated to be applicable in miniaturized sensor for medical applications.

Acknowledgements

We would like to thank the Egyptian Government and Assiut University for funding this research project. Also thanking should extend to Center of Excellence for Research and Education on Complex Functional Mechanical Systems (COE program of the Ministry of Education, Culture, Sports, Science and Technology, Japan).

References

- 1 M. E. H. Eltaib and J. R. Hewit: *Mechatronics* **13** (2003) 1163.
- 2 S. Omata and Y. Terunuma: *Sens. Actuators A* **35** (1992) 9.
- 3 R. Sedaghati, J. Dargahi and H. Singh: *Int. J. Solids and Structures* **42** (2005) 5872.

- 4 J. Engel., J. Chen, Z. Fan and C. Liu: *Sens. Actuators A* **117** (2005) 50.
- 5 M. Shikida, T. Shimizu, K. Sato and K. Itoigawa: *Sens. Actuator A* **103** (2003) 213.
- 6 F. J. Carter, T. G. Frank, P. J. Davies, D. MacLean, and A. Cuschieri: *Medical Image Analysis* **5** (2001) 231.
- 7 G. Oleg, P. Marayong and A. M. Okamura: *Computer Aided Surgery* **9** (2004) 243.
- 8 K. Chinzei, K. Miller, K. Homma and K. Hyodo: 36th Conf. Japan Soc. Med. Electronics Biol. Eng. BME 1997 (Japanese J. Med. Electronics Biol. Eng., 1997) p. 316.
- 9 M. Farshad, M. Barbezat, P. Flüeler, F. Schmidlin, P. Graber and P. Niederer: *J. Biomechanics* **32** (1999) 417.
- 10 J. Kim, B.K. Tay, N. Stylopoulos, D.W. Rattner and M.A. Srinivasan : 6th International Medical Image Computing & Computer Assisted Intervention 2003 (MICCAI, Montreal, 2003) p. 206.
- 11 Y. P. Zheng and A. F. T. Mak: *IEEE Trans. Biomed. Eng.* **43** (1996) 912.
- 12 Y. Husegawa, H. Sasaki, T. Ando, M. Shikida, K. Sato , K. Itoigawd: *MEMS 2005 (IEEE, 2005)* p. 275.
- 13 M. E. H. Eltaib: *Oscillating Tactile Probe for Robotics and Medical Applications* (Ph.D. thesis, University of Dundee, UK, October 2001) p. 73.
- 14 K. Miller, K. Chinzei, G. Orssengo and P. Bednarz: *J. Biomech* **33** (2000) 1369.